

Supporting Information for "Numerical Simulations of Hydraulic Redistribution Across Climates: The Role of the Root Hydraulic Conductivities."

DOI: 10.1002/2014WR016509

Juan C. Quijano¹, and Praveen Kumar^{1,2}

Contents of this file

1. Table S1:
2. Figures S1 to S4:

Introduction

This supporting information provides additional information to the main article. Table S1 provides a list of the most dominant species at all the sites. Figure S1 shows the leaf area index at all the sites. Figure S2 and S3 are the same as Figure 3 in the main article, but they include all the sites. Similarly, Figure S4 is the same as Figure 4 in the main article but including all the sites.

¹Department of Civil and Environmental Engineering, University of Illinois, Urbana, IL 61801, USA

²Department of Atmospheric Sciences, University of Illinois, Urbana, IL 61801, USA

References

- Domingues, T. F., J. A. Berry, and J. R. Ehleringer, Parameterization of Canopy Structure and Leaf-Level Gas Exchange for an Eastern Amazonian Tropical Rain Forest (Tapajós National Forest , Pará , Brazil), *Earth Interactions*, 9(17), 2005.
- Misson, L., J. W. Tang, M. Xu, M. McKay, and A. Goldstein, Influences of recovery from clear-cut, climate variability, and thinning on the carbon balance of a young ponderosa pine plantation, *Agricultural and Forest Meteorology*, 130(3-4), 207–222, 2005.
- P. Kumar, Department of Civil and Environmental Engineering , University of Illinois at Urbana Champaign, Hydrosystems Building, Urbana, IL 61802, USA (kumar1@illinois.edu)

Table 1: List of dominant vegetation species at all the sites.

Site	Vegetation Species
Metolius	Pinus ponderosa.
Blodgett	Pinus Ponderosa. Understory species include Arctostaphylos manzanita, and Ceanothus Cordulatus.
Harvard	Quercus rubra, Acer rubrum, Betula lenta, and Tsuga canadensis.
Howland	Picea rubens, Tsuga canadensis, Abies balsamea, and Pinus strobus.
Morgan	Acer saccharum, Liriodendron tulipifera, Sassafras albidum, and Quercus alba.
Willow Creek	Acer saccharum, Tilia americana, Dirca palustris, and Adiantum pedatum.
Tapajós	Many different vegetation species. Dominant include Manilkara huberi and Hymenaea courbaril.
Austin Cary	Pinus palustris, Pinus elliotii, Serenoa repens, and Ilex glabra.
Duke	Carya tomentosa, Liriodendron tulipifera, and Liquidambar styraciflua.

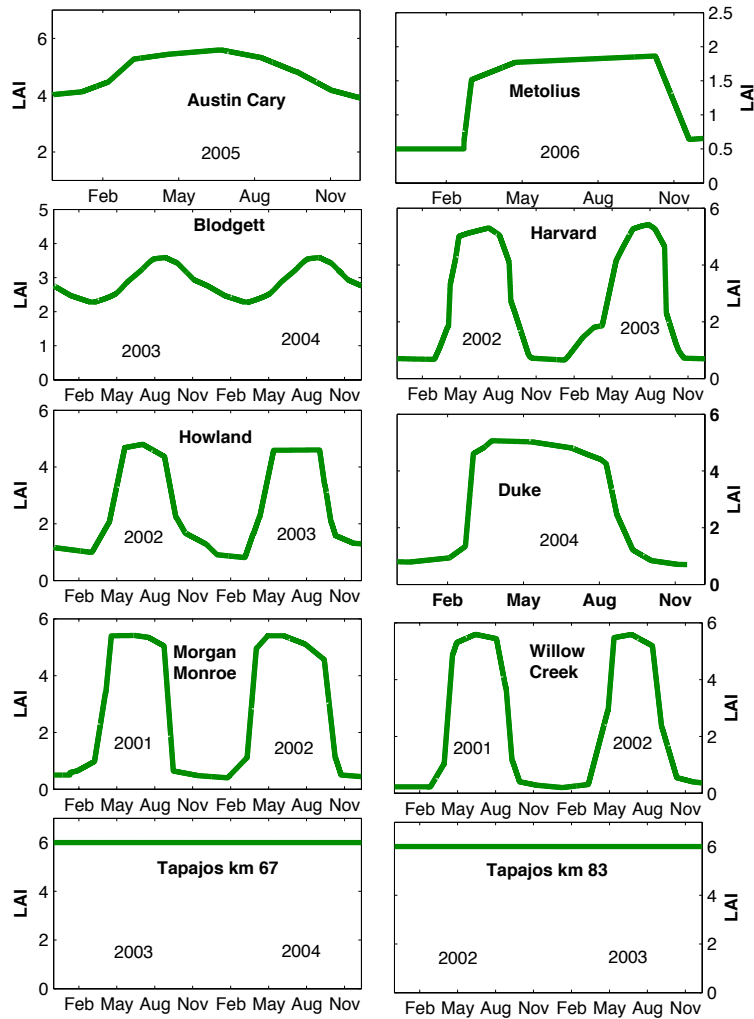


Figure S1. Leaf Area Index (LAI) for all the sites simulated in this study. In Austin Cary, Metolius Intermediate Forest, Howland Forest, Duke Forest Harwoods, Morgan Monroe, and Willow Creek Ameriflux sites the LAI was obtained from MODIS data provided by the Ameriflux Network. In Blodgett Forest Ameriflux site the LAI information was obtained by a combination of both Modis Data provided by the Ameriflux Network and *Misson et al.* [2005]. In Tapajós Km 67 and Km 83 Ameriflux sites the LAI information was obtained from *Domingues et al.* [2005], and in Harvard Forest Ameriflux site the LAI information was obtained by a combination of both Modis Data and LAI measurements provided by the Ameriflux Network. All the MODIS data was post-processed and smoothed in order to avoid numerical instabilities.

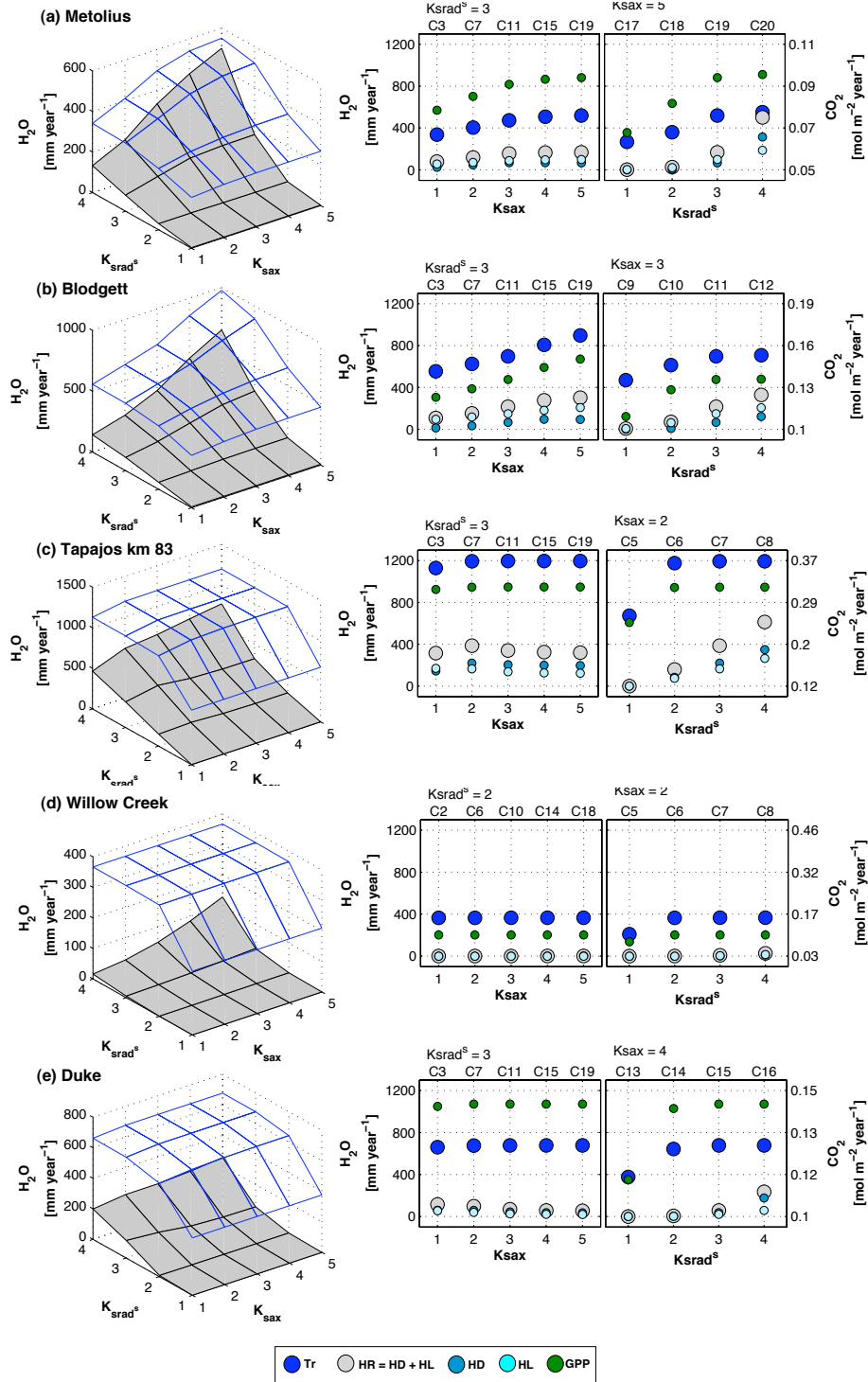


Figure S2. Effect of specific root radial hydraulic conductivity k_{srad} and specific root axial conductivity k_{sax} on the fluxes of transpiration (Tr), hydraulic redistribution (HR), hydraulic lift (HL), hydraulic descent (HD), and gross primary production (GPP) at (a) Metolius Forest, (b) Blodgett Forest, (c) Tapajós Km 83, (d) Willow Creek, (e) and Duke Forest Hardwoods.

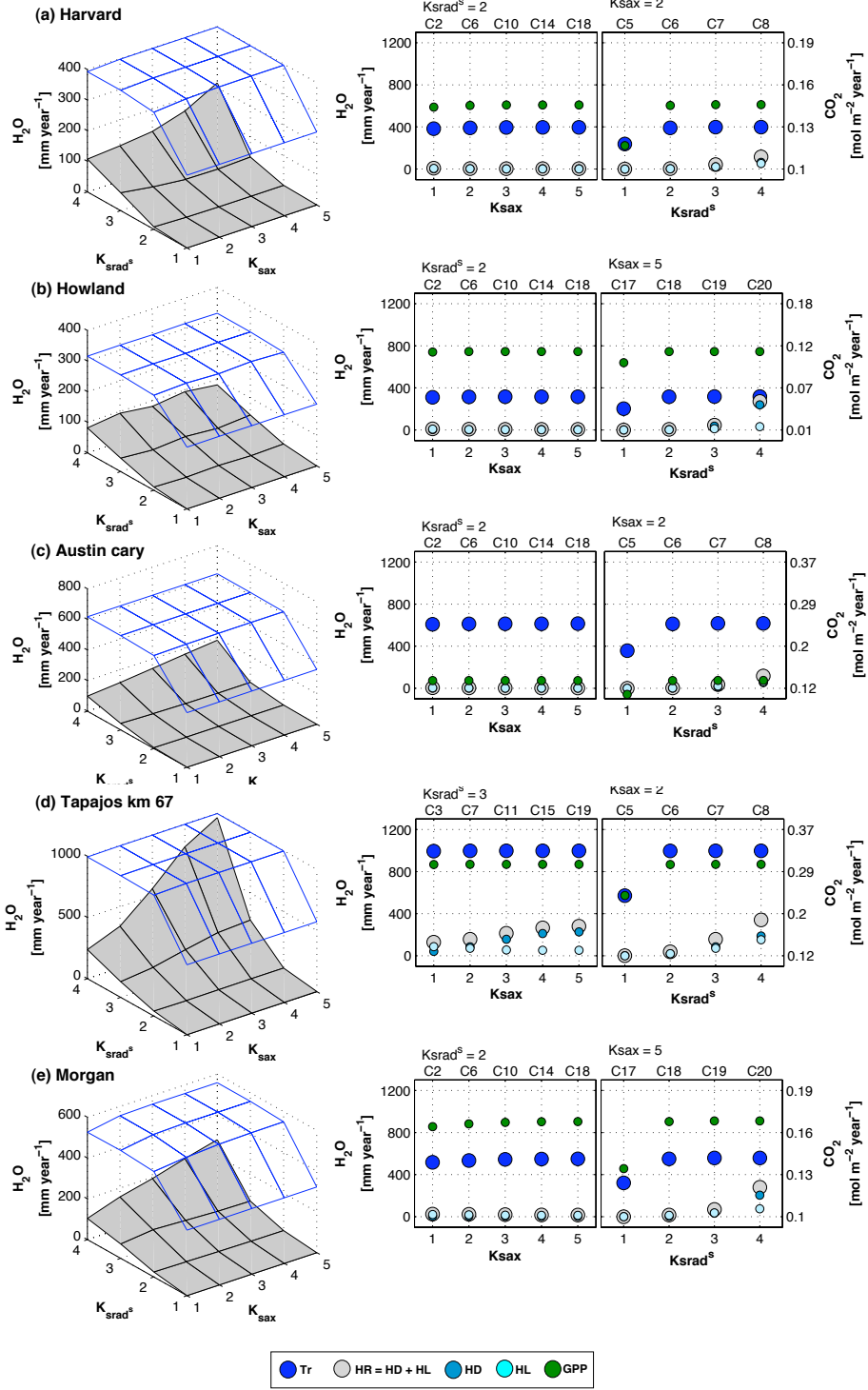


Figure S3. Effect of saturated specific root radial hydraulic conductivity K_{srad}^s and specific root axial conductivity K_{sax} on the fluxes of transpiration (Tr), hydraulic redistribution (HR), hydraulic lift (HL), hydraulic descent (HD), and gross primary production (GPP) at (a) Harvard Forest, (b) Howland Forest, (c) Austin Cary, (d) Tapajós Km 67, (e) and Morgan Monroe State Forest.

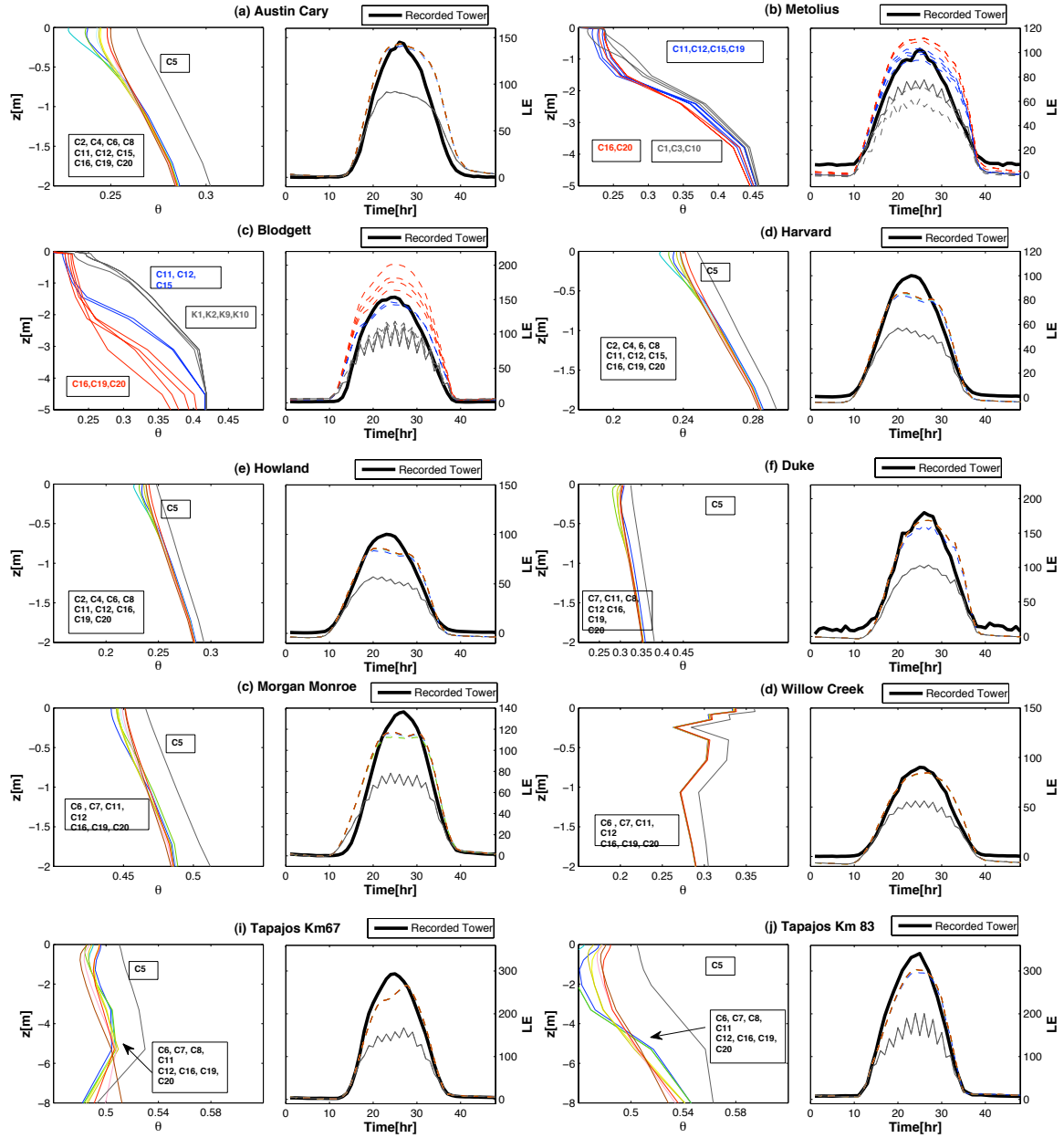


Figure S4. Average soil moisture distribution in the soil domain (left), and mean diurnal latent heat fluxes (right) for different combinations of root conductivities at all the sites included in this study.